Identifying Non-Abelian Topological Order through Minimal Entangled States

W. Zhu,[1] S. S. Gong,[1] F. D. M. Haldane,[2] and D. N. Sheng[1]
[1]Department of Physics and Astronomy, California State University, Northridge, California 91330, USA
[2]Department of Physics, Princeton University, Princeton, New Jersey 08544, USA
(Received 29 August 2013; published 4 March 2014)

The topological order is encoded in the pattern of long-range quantum entanglements, which cannot be measured by any local observable. Here we perform an exact diagonalization study to establish the non-Abelian topological order for topological band models through entanglement entropy measurement. We focus on the quasiparticle statistics of the non-Abelian Moore-Read and Read-Rezayi states on the lattice models with bosonic particles. We identify multiple independent minimal entangled states (MESs) in the ground state manifold on a torus. The extracted modular $\mathcal{S}$ matrix from MESs faithfully demonstrates the Ising anyon or Fibonacci quasiparticle statistics, including the quasiparticle quantum dimensions and the fusion rules for such systems. These findings unambiguously demonstrate the topological nature of the quantum states for these flatband models without using the knowledge of model wave functions.

DOI: 10.1103/PhysRevLett.112.096803 PACS numbers: 73.43.Cd, 03.65.Ud, 05.30.Pr

Introduction.—One of the most striking phenomena theoretically predicted in the fractional quantum Hall (FQH) system is the emergent fractionalized quasiparticles obeying Abelian [1] or non-Abelian [2–4] braiding statistics. The interchange of two Abelian quasiparticles leads to a nontrivial phase acquired by their wave function, whereas the interchange of two non-Abelian quasiparticles results in an operation of matrix to the degenerating ground state space, and the final state will depend on the order of operations being carried out. The non-Abelian quasiparticles and their braiding statistics are fundamentally important for understanding the topological order and also have potential application in topologically fault-tolerant quantum computation [5–7]. Two of the simplest states hosting the non-Abelian statistics are Moore-Read (MR) [2,8,9] and Read-Rezayi (RR) states [4,10]. In the MR and RR states, the quasiparticles satisfy the following characteristic fusion rules that specify how the quasiparticles combine and fuse into more than one type of quasiparticle [7],

$$\mathrm{MR}:\ \sigma \times \sigma = \mathbb{1} + \psi, \tag{1a}$$

$$\mathrm{RR}:\ \tau \times \tau = \mathbb{1} + \tau, \tag{1b}$$

where $\mathbb{1}$ represents the identity particle, ψ the fermion-type quasiparticle, σ the Ising anyon quasiparticle, and τ the Fibonacci quasiparticle. In general, the fusion rule of quasiparticles is encoded in the modular $\mathcal{S}$ matrix through the Verlinde formula [11–19]. Moreover, $\mathcal{S}$ also determines the quasiparticle's individual quantum dimension (d_i), statistics, and total quantum dimension ($\mathcal{D} = \sqrt{\sum_i d_i^2}$) [20,21]. Therefore, the $\mathcal{S}$ matrix plays the central role in identifying topological order and the corresponding quasiparticle property [16–19].

Although non-Abelian quasiparticles have not been definitely identified in nature, it is generally believed that they exist in the FQH systems at filling factor $\nu = 5/2$ [22] and $12/5$ [23]. To demonstrate the non-Abelian nature of quasiparticles in these states, numerical efforts have been made to show the Berry phase of quasiparticles moving adiabatically around each other [24–30]. However, the full modular $\mathcal{S}$ matrix and the corresponding fusion rules for these possible non-Abelian topological states have not been identified, which is one of the major challenges in studying the topological order of microscopic interacting systems. The topological flatband model (TFB) with bosonic particles is another promising platform to study the non-Abelian topological states [31–43], which could be realized in optical lattices or strongly interacting and frustrated condensed matter systems. For the TFB models, so far, the ground state degeneracy, entanglement spectrum, and wave function overlap have been used to identify the topological order [36,37]. The direct access of the modular matrix and non-Abelian quasiparticle statistics for these microscopic systems are highly desired, which can fully distinguish different topological states [12,19].

Recently, there is growing interest in characterizing topological order through the quantum entanglement information [20,21,44–52]. Among the recent progress, the relationship between the entanglement measurement and the modular matrix for topological nontrivial systems has been uncovered [49], which may open a new avenue to this challenging issue. The modular matrix and corresponding quasiparticle statistics have been successfully extracted through the minimal entangled states (MESs) for chiral spin liquid and the Abelian FQH states [49,50,53], which serve as direct evidence that the MES is the eigenstate of the Wilson loop operator with a definite type of quasiparticle [13,49,50]. For the non-Abelian case, as the

quasiparticles usually have different quantum dimensions and topological entanglement entropies, to target all MESs, one needs to project out the previously identified lower entropy MESs and focus on the projected Hilbert space. A recent variational quantum Monte Carlo work studied the quasiparticle statistics for a projected wave function based on MESs [54]; however, the obtained result has relatively larger error (see the Supplemental Material [55]) in reproducing the known modular matrix including each quasiparticle quantum dimension for the MR state. So far, there are no qualitatively good results presented for the RR state. Thus, it is of critical importance to clarify if the MESs can lead to the accurate identification of the modular matrix and the corresponding topological order for microscopic non-Abelian quantum states.

In this Letter, we present an exact diagonalization (ED) study of quasiparticle statistics of the possible MR and RR non-Abelian states through extracting the modular $\mathcal{S}$ matrix for TFB models [31–37] with bosonic particles at filling numbers $\nu = 1$ and $\nu = 3/2$. We map out the entanglement entropy profile for superposition states of the near-degenerating ground states and identify the global MES. We find that all other MESs can be obtained in the state space which is orthogonal to the global MES. The obtained MESs form the orthogonal and complete basis states for the modular transformation. We extract the modular $\mathcal{S}$ matrix and establish the corresponding fusion rules, which unambiguously demonstrate the Ising anyon and Fibonacci quasiparticles emerging in these systems. We show that the obtained modular matrix as a topological invariant [18] of the system remains to be universal in the whole topological phase until a quantum phase transition takes place. Thus, we establish that the MES method is effective in identifying non-Abelian topological order for microscopic interacting systems, which can be applied to different numerical studies of topological nontrivial systems.

We study the lattice boson model with longer-range hoppings, which can be generally written as

$$H = \sum_{\mathbf{r}\mathbf{r}'} [J_{\mathbf{r}\mathbf{r}'} e^{i\phi_{\mathbf{r}'\mathbf{r}}} b^\dagger_{\mathbf{r}'} b_{\mathbf{r}} + \text{H.c.}] + \sum_n \frac{U_n}{n!} \sum_{\mathbf{r}} (b^\dagger_{\mathbf{r}})^n (b_{\mathbf{r}})^n, \quad (2)$$

where $b^\dagger_{\mathbf{r}}(b_{\mathbf{r}})$ creates (annihilates) a boson at site $\mathbf{r} = (x, y)$. U_n is an on-site N-body repulsive interaction. Here we consider two representative lattice models: the Haldane model on the honeycomb (HC) lattice [31,43] and the TFB model on the square (SQ) lattice [32].

On the HC lattice, we include up to the third nearest-neighbor (NN) hopping and a nonzero ϕ_{ij} on the second NN hopping only (the net flux is zero in one unit cell), as shown in Fig. 1(a). The NN hopping is set to be $J_{\mathbf{r}\mathbf{r}'} = 1$ and the other parameters are defined the same as in Ref. [43]. On the SQ lattice [32], we select the phase

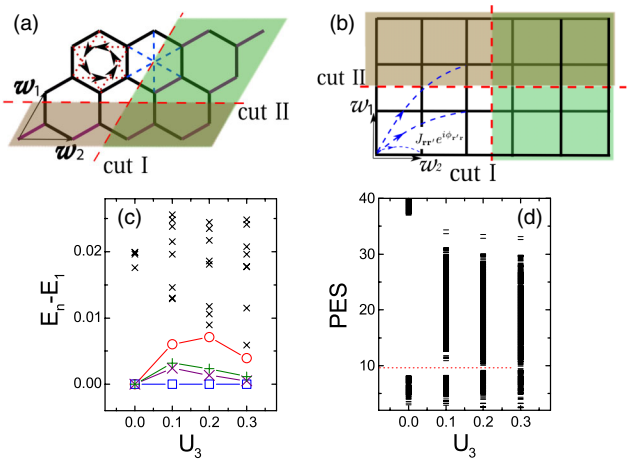

FIG. 1 (color online). (a) Haldane model on HC lattice. The red dashed and blue dashed lines represent the second NN hopping and third NN hopping, respectively. (b) SQ lattice with long-range hopping $J_{\mathbf{r}\mathbf{r}'} e^{i\phi_{\mathbf{r}'\mathbf{r}}}$ as shown by the blue dashed line. (c) Low-energy spectrum $E_n - E_1$ versus the U_3 ($U_2 = 0$, $U_{n\geq 4} = \infty$) on a 4×4 SQ lattice at $\nu = 3/2$. The four lowest eigenvalues are labeled by the blue square, purple cross, green cross, and red circle. (d) Particle entanglement spectrum (PES) for tracing out four bosons. There are 298 states below the PES gap (red dashed line) for $U_3 < 0.3$, in good agreement with the counting of quasihole excitations in the RR state.

factor $\phi_{\mathbf{r}'\mathbf{r}}$ corresponding to half flux quanta per plaquette. The amplitude of hopping satisfies a particular Gaussian form, $J_{\mathbf{r}\mathbf{r}'} = -tG(\mathbf{r} - \mathbf{r}')e^{-(\pi/4)|\mathbf{r}-\mathbf{r}'|^2}$, where $G(\mathbf{r} - \mathbf{r}') = (-1)^{(1+x-x')(1+y-y')}$ and $t = 1$ as the energy scale here. For both models, we consider a finite size system with $N_x \times N_y$ unit cells; the filling factor of the lower band is $\nu = N_p/N_s$, where N_p is the boson number, and N_s is number of single-particle states in the flatband.

We first obtain the low-energy spectrum of the SQ model at filling number $\nu = 3/2$ and $\nu = 1$ (see the Supplemental Material [55]). For $\nu = 3/2$, we set $U_{n\geq 4} = \infty$ so that only three bosons can go to the same lattice site, which is effectively equivalent to a spin-$\frac{3}{2}$ system. Because of much larger Hilbert space than the conventional hard-core boson systems, the largest size we can deal with is limited to 4×4 for $\nu = 3/2$. The RR (MR) state is the exact ground state on the SQ lattice for $U_3 = 0$ ($U_2 = 0$) at $\nu = 3/2$ ($\nu = 1$) [32]. Here, we find strong numerical evidence that the $\nu = 3/2$ RR state ($\nu = 1$ MR state) extends to finite U_3 (U_2) (see the Supplemental Material [55]) on the SQ lattice. As shown in Figs. 1(c) and 1(d), at the smaller U_3 side, we find robust fourfold degeneracy of ground states on a torus and the right counting rule of quasiparticle excitations for the RR state [56]. Our focus is to characterize the quasiparticle statistics of the above non-Abelian states through calculating the modular $\mathcal{S}$ matrix.

To address the quasiparticle statistics, we first obtain the quasiparticle eigenstates through determining the MESs on a torus [49]. The entanglement entropy is defined as

$S = -Tr\rho_A \log \rho_A$, where the reduced density matrix ρ_A is obtained through partitioning the full system into two subsystems A and B and tracing out the subsystem B. Here we consider two noncontractible bipartitions on torus geometry (cut I and cut II) [Figs. 1(a) and 1(b)], which is along the lattice vectors w_1, w_2, respectively.

Moore-Read state at $\nu = 1$.—We first study the HC lattice at $U_2 = 0$, where it is found a stable $\nu = 1$ MR state with threefold quasidegeneracy of ground states on a torus [43]. We denote the three ground states from the ED calculation as $|\xi_j\rangle$, (with $j = 1, 2, 3$) [43]. Now we form the general superposition states as

$$|\Psi_{(c_1,c_2,\phi_2,\phi_3)}\rangle = c_1|\xi_1\rangle + c_2 e^{i\phi_2}|\xi_2\rangle + c_3 e^{i\phi_3}|\xi_3\rangle,$$

where c_1, c_2, c_3, ϕ_2, ϕ_3 are real superposition parameters. For each state $|\Psi\rangle$, we construct the reduced density matrix and obtain the corresponding entanglement entropy. We optimize values of $c_i \in [0, 1]$ and $\phi_i \in [0, 2\pi]$ to minimize the entanglement entropy. In Fig. 2(a), we show the entropy profile at optimized parameters (ϕ_2^o, ϕ_3^o) for MESs on the HC lattice. Here we draw the $-S$ in the surface and contour plots so that the peaks in entropy show up clearly representing the minimums of S. In Fig. 2(a), we find several peaks (entropy valleys) in $c_1 - c_2$ space. The first peak (red arrow) relates to the first (global) MES $|\Xi_1^I\rangle$. After determining $|\Xi_1^I\rangle$, we search for the states with minimal entropy in the state space orthogonal to $|\Xi_1^I\rangle$ as shown in Fig. 2(b). The second and the third MESs are shown by green and blue arrows (the two states labeled by blue arrows are equivalent), which are separately located in different entropy valleys, as shown in Fig. 2(a). We find that the first two MESs have almost the same entropy value, indicating they are, indeed, topologically equivalent with the same quantum dimension. We calculate the entropy difference δS between the third MES and the average of the first two MESs to extract the information of the quantum dimension of the third quasiparticle. As listed in Table I,

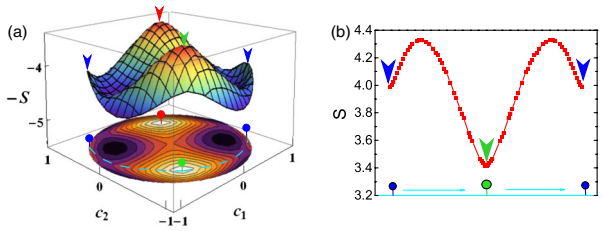

FIG. 2 (color online). (a) Surface and contour plots of the entanglement entropy ($-S$) of $|\Psi_{c_1,c_2,\phi_2,\phi_3}\rangle$ on a 3×4 HC lattice at $\nu = 1$ for $U_2 = 0$. We show the entropy profile versus c_1, c_2 ($c_3 = \sqrt{1 - c_1^2 - c_2^2}$) by setting optimized $\phi_2^o = 1.26\pi$, $\phi_3^o = 0.40\pi$. Three nearly orthogonal MESs are marked by red, green, and blue arrows (dots) in the surface (contour) plot. The cyan dashed line represents the states orthogonal to the first MES (red dot). (b) Entropy for the states along the cyan dashed line as shown in (a). All calculations are for the partition along cut I.

nonzero $\delta S \approx 0.576$ implies the quantum dimension $d > 1$ for the third quasiparticle state [20,21], in agreement with the theoretical expectation for a MR state. We also search for MESs for the SQ lattice (see the Supplemental Material [55]) and find similar results as listed in Table I.

To extract the topological information of the quantum states from MESs, we obtain the overlap between the MESs for two noncontractible partition directions, which gives rise to the modular matrix $\mathcal{S} = \langle \Xi^{II} | \Xi^{I} \rangle$ [49],

$$\mathcal{S} \approx \frac{1}{2.033} \begin{pmatrix} 1.000 & 1.026 & 1.441 \\ 1.000 & 1.026 & -1.441 \\ 1.463 & -1.409 & 0.000 \end{pmatrix}, \quad (3)$$

for the HC lattice ($U_2 = 0$), and we find a very similar result for the SQ lattice (see the Supplemental Material [55]). At $\nu = 1$, the bosonic MR state is described by $SU(2)_2$ Chern-Simons theory, which can be further confirmed by identifying the chiral central charge to be $c_- = 3/2$ based on the total Chern number $C = 3$ of the three near-degenerate ground states [55,57]. Indeed, the numerical modular matrices we obtain are quite close to the theoretical result from $SU(2)_2$ Chern-Simons theory [13–15],

$$\mathcal{S} = \frac{1}{2} \begin{pmatrix} 1 & 1 & \sqrt{2} \\ 1 & 1 & -\sqrt{2} \\ \sqrt{2} & -\sqrt{2} & 0 \end{pmatrix},$$

which determines the quasiparticle quantum dimension as $d_{\mathbb{1}} = 1$, $d_\psi = 1$, $d_\sigma = \sqrt{2}$, $\mathcal{D} = 2$ and the nontrivial fusion rule in Eq. (1a). From Eq. (3), we obtain $d_\sigma^{\mathrm{HC}} \approx 1.463$, $\mathcal{D}^{\mathrm{HC}} \approx 2.033$ for the HC lattice (and $d_\sigma^{\mathrm{SQ}} \approx 1.392$, $\mathcal{D}^{\mathrm{SQ}} \approx 1.961$ for the SQ lattice [see the Supplemental Material [55]]). Another striking point is that $\mathcal{S}_{33} \sim 0$, which indicates that the two σ quasiparticles annihilate each other and fuse into other quasiparticles. To demonstrate this nontrivial behavior, we extract the fusion rule related to the third quasiparticle from the numerical $\mathcal{S}$ matrix through the Verlinde formula [11] $a \times b = \sum_c N_{ab}^c c$ where $N_{ab}^c = \sum_m \mathcal{S}_{am}\mathcal{S}_{bm}\mathcal{S}_{mc}^*/\mathcal{S}_{1m}$,

$$\mathrm{HC}: \sigma \times \sigma \approx 1.005\mathbb{1} + 1.056\psi + 0.096\sigma, \quad (4a)$$

$$\mathrm{SQ}: \sigma \times \sigma \approx 0.951\mathbb{1} + 0.959\psi + 0.004\sigma, \quad (4b)$$

TABLE I. Entropy of MESs for $\nu = 1$ and $\nu = 3/2$. S_i represents the entropy of the ith MES. For $\nu = 1$, we use $\delta S = S_3 - (S_2 + S_1)/2$. For $\nu = 3/2$, $\delta S = (S_3 + S_4)/2 - (S_1 + S_2)/2$. δS^* is analytic prediction [20].

ν	Lattice size	S_1	S_2	S_3	S_4	δS	δS^*	$\delta S/\delta S^*$
1	HC 3×4	3.416	3.416	3.991	$\cdots$	0.576	0.693	0.831
1	SQ 4×4	2.546	2.924	3.357	$\cdots$	0.622	0.693	0.897
1	SQ 4×6	2.528	2.971	3.443	$\cdots$	0.694	0.693	1.001
$\frac{3}{2}$	SQ 4×4	3.168	3.732	4.157	4.417	0.837	0.961	0.871

which agrees excellently with the fusion rule of the MR state [Eq. (1a)]. Both the $d_\sigma \approx \sqrt{2}$ and the characteristic fusion rule Eqs. (4a) and (4b) unambiguously demonstrate the third quasiparticle σ representing an Ising anyon quasiparticle. The fusion rule represents two ways to fuse two σ quasiparticles; therefore, each pair of σ quasiparticles can act as a qubit for quantum computation [7].

Read-Rezayi state at $\nu = 3/2$.—We turn to study the possible non-Abelian phase on the SQ lattice at $\nu = 3/2$ and detect the Fibonacci quasiparticle statistics emerging in this state. Following the similar route for MR at $\nu = 1$, we search for the MESs in the space of the ground state manifold using the following general wave functions:

$$|\Psi\rangle = c_1|\xi_1\rangle + c_2 e^{i\phi_2}|\xi_2\rangle + c_3 e^{i\phi_3}|\xi_3\rangle + c_4 e^{i\phi_4}|\xi_4\rangle,$$

where c_i and ϕ_i are the superposition parameters and $|\xi_j\rangle$ ($j = 1, 2, 3, 4$) are four ground states from the ED calculation. We optimize the superposition parameters c_i, ϕ_i to minimize the entanglement entropy. In Fig. 3(a), we show the global MES $|\Xi_1^I\rangle$ in parameter space as labeled by the black arrow. The other MESs $|\Xi_i^I\rangle$ ($i = 2, 3, 4$) are determined in the parameter space orthogonal to $|\Xi_1^I\rangle$ [Fig. 3(b)]. The entropies of the last two MESs are different from the lowest two MESs, as listed in Table I, which is consistent with the non-Abelian behavior of the quasiparticles. However, we also notice some finite size effect as all the four entropies are different.

For the $\nu = 3/2$ bosonic RR state, the edge conformal field theory is captured by the $SU(2)_3$ Wess-Zumino-Witten model [13,15–17], whose modular matrix can be effectively described by a non-Abelian $k = 3$ $\mathbb{Z}_k$-parafermion part coupled with an Abelian semion part as

$$\mathcal{S} = \mathcal{S}_{pf} \otimes \mathcal{S}_{U(1)} = \frac{1}{\sqrt{2+\phi}} \begin{pmatrix} 1 & \phi \\ \phi & -1 \end{pmatrix} \otimes \frac{1}{\sqrt{2}} \begin{pmatrix} 1 & 1 \\ 1 & -1 \end{pmatrix},$$

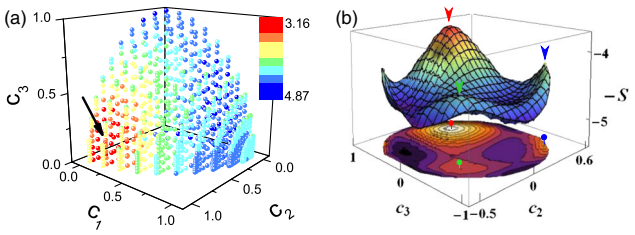

FIG. 3 (color online). (a) The entropy profile of wave function $|\Psi\rangle$ on a 4×4 SQ lattice ($U_2 = U_3 = 0$) at $\nu = 3/2$ in $c_1 - c_2 - c_3$ space by setting optimized $\phi_2^o = 0.90\pi$, $\phi_3^o = 0.46\pi$, $\phi_4^o = 0.68\pi$. The color of the dots represents the magnitude of the entropy. The first MES is indicated by the black arrow. (b) The entropy profile versus $c_2 - c_3$ in the space orthogonal to the first MES. The second, third, and fourth MESs are labeled by red, green, and blue arrows and dots, respectively. The calculation is for a bipartition system along the cut-I direction.

where $\phi = (1 + \sqrt{5}/2)$ is the golden ratio number. As a comparison, we obtain the numerical modular matrix by calculating the overlap between the MESs along cuts I and II,

$$\mathcal{S} \approx \mathcal{S}_{pf} \otimes \mathcal{S}_{U(1)} + 10^{-2} \times \begin{pmatrix} 4.3 & -3.4 & -0.4 & 1.1 \\ -2.7 & -3.1 & -0.9 & -0.1 \\ 2.1 & -0.8 & 2.4 & -0.7 \\ 0.0 & -1.0 & -0.1 & -1.9 \end{pmatrix}, \tag{5}$$

which agrees with the analytic prediction (with a finite size correction of the order of 10^{-2}). The modular matrix $\mathcal{S}_{pf}$ signals a Fibonacci quasiparticle including the quantum dimension $d_\tau = \phi \approx 1.618$ and the related fusion rule as shown in Eq. (1b). Two Fibonacci quasiparticles may fuse into an identity or a Fibonacci quasiparticle, which is similar to two $SU(2)$ spin-1/2 particles combining to either spin-1 or spin-0 total spin [58]. Using this property, Fibonacci quasiparticles may be capable of performing universal topological quantum computing [7].

Quantum phase transition.—By tuning the interaction U_n, we can drive a quantum phase transition from the non-Abelian state to other quantum phases [43,55]. A natural question is how the MESs and the related modular $\mathcal{S}$ matrix evolve around the quantum phase transition region. Here we study the SQ lattice model at $\nu = 1$ as an example in which the quantum phase transition occurs around $0.3 \leq U_2^c \leq 0.4$ (see the Supplemental Material [55]). In the MR phase ($U_2 = 0.1$), we find that the entropy profile of the superposition state has three valleys labeled by I, II, and III, as shown in Fig. 4(a). The three orthogonal MESs are located in the above three valleys, respectively. The resulting modular matrix remains close to the theoretical one for the MR state,

$$\mathcal{S} = \frac{1}{1.965} \begin{pmatrix} 1.000 & 1.041 & 1.316 \\ 1.006 & 0.888 & -1.448 \\ 1.334 & -1.440 & 0.028 \end{pmatrix}.$$

We have also found that the $\mathcal{S}$ faithfully represents the quasiparticle information for $U_2 < 0.3$ with the accuracy

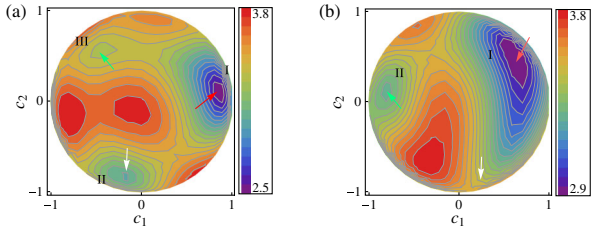

FIG. 4 (color online). The entropy of superposition state $|\Psi\rangle$ in $c_1 - c_2$ space ($c_3 = \sqrt{1 - c_1^2 - c_2^2}$) for (a) $U_2 = 0.1$ and (b) $U_2 = 0.5$ by setting optimized ϕ_2, ϕ_3 at $\nu = 1$ on the SQ lattice.

error less than or around 10% (see the Supplemental Material [55]). Only in the transition region ($U_2 \sim 0.3$–0.4) the accuracy error jumps up. After the quantum phase transition at $U_2 = 0.5 > U_2^c$, we can only find two entropy valleys in the entropy map, as labeled by I, II in Fig. 4(b), which relates to the first two MESs. The third possible MES state (labeled by the white arrow) determined by the orthogonality relation, actually is not a local minimum. We continue to use these MESs as basis states to obtain the modular $\mathcal{S}$ matrix,

$$\mathcal{S} = \frac{1}{3.731}\begin{pmatrix} 1.000 & 2.873 & 2.037 \\ 2.899 & 0.750 & 2.354 \\ 2.015 & 2.354 & 2.082 \end{pmatrix},$$

which deviates significantly from the MR $\mathcal{S}$ matrix. In particular, the quasiparticle fusion rule and statistics have changed with $\mathcal{S}_{33}$ deviating from zero (see the Supplemental Material [55]), which demonstrates the disappearance of the MR phase.

Summary and discussion.—We have numerically studied the non-Abelian quasiparticle statistics in the lattice boson models which manifest the MR and RR non-Abelian states at filling factor $\nu = 1$ and $\nu = 3/2$, respectively. Our work provides the first convincing demonstration of quasiparticle fusion rules and statistics in microscopic TFB models without using the knowledge of model wave functions. The obtained modular $\mathcal{S}$ matrix faithfully represents Ising anyon and Fibonacci quasiparticle statistics as the fingerprint of the non-Abelian topological order. Our work also supports that each MES is the eigenstate of the Wilson loop operator with a definite type of quasiparticle, from which the topological order can be extracted. We are currently developing a numerical method in density-matrix renormalization group simulations to target different MESs by projecting out the previously identified lower entropy MESs, which we believe will become a useful tool for detecting the full information of the topological order through modular matrix simulation in larger interacting systems.

This work is supported by the U.S. Department of Energy, Office of Basic Energy Sciences under Grant No. DE-FG02-06ER46305 (W. Z., D. N. S.), the NSF Grant No. DMR-0906816 (S. S. G.), and the Princeton MRSEC Grant No. DMR-0819860 (F. D. M. H.). D. N. S. also acknowledges the travel support by the Princeton MRSEC.

Note added.—After we submitted this paper, we noticed a similar result for a modular matrix of the MR state in an unpublished work [59].

[1] R. B. Laughlin, Phys. Rev. Lett. **50**, 1395 (1983).
[2] G. Moore and N. Read, Nucl. Phys. **B360**, 362 (1991).
[3] M. Greiter, X. G. Wen, and F. Wilczek, Phys. Rev. Lett. **66**, 3205 (1991).
[4] N. Read and E. Rezayi, Phys. Rev. B **59**, 8084 (1999).
[5] A. Y. Kitaev, Ann. Phys. (Amsterdam) **303**, 2 (2003).
[6] S. Das Sarma, M. Freedman, and C. Nayak, Phys. Rev. Lett. **94**, 166802 (2005).
[7] C. Nayak, S. H. Simon, A. Stern, M. Freedmanm, and S. D. Sarma, Rev. Mod. Phys. **80**, 1083 (2008).
[8] R. H. Morf, Phys. Rev. Lett. **80**, 1505 (1998).
[9] E. H. Rezayi and F. D. M. Haldane, Phys. Rev. Lett. **84**, 4685 (2000).
[10] E. H. Rezayi and N. Read, Phys. Rev. B **79**, 075306 (2009).
[11] E. Verlinde, Nucl. Phys. **B300**, 360 (1988).
[12] X. G. Wen, Int. J. Mod. Phys. B **04**, 239 (1990).
[13] S. Dong, E. Fradkin, R. G. Leigha, and S. Nowling, J. High Energy Phys. 05 (2008) 016.
[14] E. Rowell, R. Stong, and Z. H. Wang, Commun. Math. Phys. **292**, 343 (2009).
[15] P. Fendley, M. P. A. Fisher, and C. Nayak, J. Stat. Phys. **126**, 1111 (2007).
[16] P. Bonderson, K. Shtengel, and J. K. Slingerland, Phys. Rev. Lett. **97**, 016401 (2006).
[17] E. Ardonne, E. J. Bergholtz, J. Kailasvuori, and E. Wikberg, J. Stat. Mech. (2008) P04016.
[18] F. A. Bais and J. C. Romers, New J. Phys. **14**, 035024 (2012).
[19] X. G. Wen, arXiv:1212.5121.
[20] A. Kitaev and J. Preskill, Phys. Rev. Lett. **96**, 110404 (2006).
[21] M. Levin and X.-G. Wen, Phys. Rev. Lett. **96**, 110405 (2006).
[22] R. Willett, J. P. Eisenstein, H. L. Stormer, D. C. Tsui, A. C. Gossard, and J. H. English, Phys. Rev. Lett. **59**, 1776 (1987).
[23] J. S. Xia, W. Pan, C. L. Vicente, E. D. Adams, N. S. Sullivan, H. L. Stormer, D. C. Tsui, L. N. Pfeiffer, K. W. Baldwin, and K. W. West, Phys. Rev. Lett. **93**, 176809 (2004).
[24] G. S. Jeon, K. L. Graham, and J. K. Jain, Phys. Rev. Lett. **91**, 036801 (2003).
[25] Y. Tserkovnyak and S. H. Simon, Phys. Rev. Lett. **90**, 016802 (2003).
[26] M. Baraban, G. Zikos, N. Bonesteel, and S. H. Simon, Phys. Rev. Lett. **103**, 076801 (2009).
[27] E. Prodan and F. D. M. Haldane, Phys. Rev. B **80**, 115121 (2009).
[28] V. Lahtinen and J. K. Pachos, New J. Phys. **11**, 093027 (2009).
[29] A. T. Bloukbasi and J. Vala, New J. Phys. **14**, 045007 (2012).
[30] E. Kapit, P. Ginsparg, and E. Mueller, Phys. Rev. Lett. **108**, 066802 (2012).
[31] F. D. M. Haldane, Phys. Rev. Lett. **61**, 2015 (1988).
[32] E. Kapit and E. Mueller, Phys. Rev. Lett. **105**, 215303 (2010).
[33] E. Tang, J. W. Mei, and X. G. Wen, Phys. Rev. Lett. **106**, 236802 (2011).
[34] T. Neupert, L. Santos, C. Chamon, and C. Mudry, Phys. Rev. Lett. **106**, 236804 (2011).
[35] K. Sun, Z. C. Gu, H. Katsura, and S. Das Sarma, Phys. Rev. Lett. **106**, 236803 (2011).

[36] D. N. Sheng, Z. C. Gu, K. Sun, and L. Sheng, Nat. Commun. **2**, 389 (2011).
[37] N. Regnault and B. A. Bernevig, Phys. Rev. X **1**, 021014 (2011).
[38] Y. -F. Wang, Z.-C. Gu, C.-D. Gong, and D. N. Sheng, Phys. Rev. Lett. **107**, 146803 (2011).
[39] S. A. Parameswaran, R. Roy, and S. L. Sondhi, Phys. Rev. B **85**, 241308(R) (2012).
[40] M. Barkeshli and X.-L. Qi, Phys. Rev. X **2**, 031013 (2012).
[41] N. R. Cooper, N. K. Wilkin, and J. M. F. Gunn, Phys. Rev. Lett. **87**, 120405 (2001).
[42] N. R. Cooper and J. Dalibard, Phys. Rev. Lett. **110**, 185301 (2013).
[43] Y. F. Wang, H. Yao, Z. C. Gu, C. D. Gong, and D. N. Sheng, Phys. Rev. Lett. **108**, 126805 (2012).
[44] M. Haque, O. Zozulya, and K. Schoutens, Phys. Rev. Lett. **98**, 060401 (2007).
[45] S. V. Isakov, M. B. Hastings, and R. G. Melko, Nat. Phys. **7**, 772 (2011).
[46] H. C. Jiang, Z. H. Wang, and L. Balents, Nat. Phys. **8**, 902 (2012).
[47] H. Li and F. D. M. Haldane, Phys. Rev. Lett. **101**, 010504 (2008).
[48] A. M. Lauchli, E. J. Bergholtz, J. Suorsa, and M. Haque, Phys. Rev. Lett. **104**, 156404 (2010).
[49] Y. Zhang, T. Grover, A. Turner, M. Oshikawa, and A. Vishwanath, Phys. Rev. B **85**, 235151 (2012).
[50] L. Cincio and G. Vidal, Phys. Rev. Lett. **110**, 067208 (2013).
[51] H. H. Tu, Y. Zhang, and X. L. Qi, Phys. Rev. B **88**, 195412 (2013).
[52] M. P. Zaletel, R. S. K. Mong, and F. Pollmann, Phys. Rev. Lett. **110**, 236801 (2013).
[53] W. Zhu, D. N. Sheng, and F. D. M. Haldane, Phys. Rev. B **88**, 035122 (2013).
[54] Y. Zhang and A. Vishwanath, Phys. Rev. B **87**, 161113(R) (2013).
[55] See the Supplemental Material at http://link.aps.org/supplemental/10.1103/PhysRevLett.112.096803 for results and additional discussion about the evolution of the energy spectrum, entanglement spectrum, and modular matrix for non-Abelian MR state at filling factor $\nu = 1$on an SQ lattice when the quantum phase transition occurs.
[56] B. A. Bernevig and N. Regnault, Phys. Rev. B **85**, 075128 (2012).
[57] A. Y. Kitaev, Ann. Phys. (Amsterdam) **321**, 2 (2006).
[58] A. Feiguin, S. Trebst, A. W. W. Ludwig, M. Troyer, A. Kitaev, Z. Wang, and M. H. Freedman, Phys. Rev. Lett. **98**, 160409 (2007).
[59] http://media.scgp.stonybrook.edu/presentations/20130614_2_cincio.pdf.